



Published in final edited form as:

Bioorg Med Chem. 2011 December 15; 19(24): 7338–7348. doi:10.1016/j.bmc.2011.10.062.

Time-dependent botulinum neurotoxin serotype A metalloprotease inhibitors

Bing Li^a, Steven C. Cardinale^a, Michelle M. Butler^a, Ramdas Pai^a, Jonathan E. Nuss^b, Norton P. Peet^a, Sina Bavari^b, and Terry L. Bowlin^a

^aMicrobiotix, Inc., One Innovation Drive, Worcester, MA 01605, USA

^bUnited States Army Medical Research Institute of Infectious Diseases, Fort Detrick, Frederick, MD 21702, USA

Abstract

Botulinum neurotoxins (BoNTs) are the most lethal of biological substances, and are categorized as class A biothreat agents by the Centers for Disease Control and Prevention. There are currently no drugs to treat the deadly flaccid paralysis resulting from BoNT intoxication. Among the seven BoNT serotypes, the development of therapeutics to counter BoNT/A is a priority (due to its long half-life in the neuronal cytosol and its ease of production). In this regard, the BoNT/A enzyme light chain (LC) component, a zinc metalloprotease responsible for the intracellular cleavage of synaptosomal-associated protein of 25 kDa, is a desirable target for developing post-BoNT/A intoxication rescue therapeutics. In an earlier study, we reported the high throughput screening of a library containing 70,000 compounds, and uncovered a novel class of benzimidazole acrylonitrile-based BoNT/A LC inhibitors. Herein, we present both structure-activity relationships and a proposed mechanism of action for this novel inhibitor chemotype.

Keywords

Botulinum neurotoxin serotype A; Benzimidazole acrylonitrile; Structure-activity relationships; Molecular modeling; Time-dependent inhibition

1. Introduction

Botulinum neurotoxins (BoNTs) are among the most potent of known biological toxins^{1, 2}, and are listed as category A biothreat agents by the Centers for Disease Control and Prevention. BoNTs are easily produced and may be delivered via an aerosol route^{2–4}. Consequently, these toxins represent a serious threat to both military personnel and civilians^{5–7}. Moreover, BoNTs are now widely used during both superficial cosmetic treatments and to ameliorate a range of physical ailments^{3, 8–15}, making their attainment, misuse, and/or adverse side effects¹⁶ more likely. Importantly, the currently available BoNT toxoid vaccine, as well as experimental preventative antibodies, cannot counter postneuronal internalization of these toxins. This is a seminal point, as it is likely that BoNT-poisoned individuals will seek medical attention only after clinical symptoms of intoxication manifest

© 2011 Elsevier Ltd. All rights reserved.

Correspondence to: Bing Li.

Publisher's Disclaimer: This is a PDF file of an unedited manuscript that has been accepted for publication. As a service to our customers we are providing this early version of the manuscript. The manuscript will undergo copyediting, typesetting, and review of the resulting proof before it is published in its final citable form. Please note that during the production process errors may be discovered which could affect the content, and all legal disclaimers that apply to the journal pertain.

(e.g., life-threatening paralysis). Currently, critical care mechanical ventilation is the only treatment option once neurons have been intoxicated and diaphragm muscles cease to function. However, long-term mechanical ventilation would be impractical for treating large numbers of intoxicated individuals. Therefore, there is an urgent need to identify and develop low molecular weight, non-peptidic BoNT inhibitors that will serve as both prophylactics and post-exposure 'rescue' therapeutics.

Of the seven BoNT serotypes (A–G), A, B, and E are known to cause botulism in humans^{1, 17}, with the BoNT/A/LC metalloprotease exhibiting the longest duration of activity in the neuronal cytosol^{18–20}. Hence, the vast majority of research to develop inhibitors to counter BoNT intoxication postneuronal internalization has focused on this LC serotype. Structurally, BoNT/A is composed of a 100 kDa heavy chain (HC) and a 50 kDa light chain (LC), which are joined by a disulfide bridge (until LC release upon neuronal internalization)^{21, 22}. The LC component is a zinc-dependent endopeptidase.

Botulinum neurotoxin neuronal intoxication involves a stepwise process of cell surface binding, receptor-mediated endocytosis, pH-induced translocation, and cytosolic metalloendoprotease activity²². The HC serves as the toxin delivery system, as it binds specific neuronal surface receptors and translocates the LC into the cell cytosol via an endosomal mechanism. Once inside the cytosol, the BoNT/A/LC cleaves a 25 kDa synaptosomal-associated protein (SNAP-25)²³, a component of the SNARE protein complex^{24, 25}, which is responsible for transporting acetylcholine into neuromuscular junctions. The BoNT/A LC-mediated cleavage of SNAP-25 inhibits this neuronal function, to produce flaccid paralysis that can potentially lead to respiratory failure and death.

As indicated above, the identification and development of BoNT/A LC inhibitors is a high priority²⁶. To this end, a substrate-to-inhibitor strategy was used to generate a potent peptide derivative, namely, 2-mercapto-3-phenylpropionyl-RATKML, which inhibits the BoNT/A LC with a K_i value of 330 nM^{27–30}. Subsequently, a similar strategy was employed by Sukonpan *et al.*³¹ to develop 17-mer BoNT/A LC peptide inhibitors, the most active of which was an α -mercapto amide derivative possessing a K_i value of 300 nM³¹. Moreover, several high throughput screening (HTS) campaigns to identify small molecule inhibitors of the BoNT/A LC have been conducted, and various chemotypes have been identified. Burnett *et al.*^{4, 32, 33} identified a non-Zn(II) coordinating BoNT/A LC indole-based bis-amidine inhibitor (NSC 240898) via a combination of HTS and subsequent pharmacophore-based database mining. The chemical optimization of NSC 240898 (**1**, Figure 1) has produced a generation of inhibitors represented by compounds **2** and **3** (Figure 1), both of which are more potent than **1**, which are enzyme specific and provide SNAP-25 protection in a chick neuronal assay^{34, 35, 36}. Additionally, Burnett and co-workers have employed their pharmacophore-based approach to discover and/or design several other, chemically diverse, non-Zn(II)-coordinating small molecule BoNT/A LC inhibitors possessing low μ M to sub- μ M K_i values^{37–40}. Park *et al.*⁴¹ have reported the identification of a novel class of Zn(II)-coordinating thiophene ketone-based BoNT/A LC inhibitors ($K_i \geq 12 \mu$ M) employing computer-aided drug design, and have used synthetic modifications to improve the potencies ($<1 \mu$ M) of these molecules^{42, 43}. Boldt *et al.*⁴⁴ have reported the synthesis of a Zn(II)-coordinating 2,4-dichlorocinnamic hydroxamic acid BoNT/A LC inhibitor that is reported to possess sub- μ M *in vitro* activity, but possesses very minimal activity *in vivo*⁴⁵. Furthermore, a series of benzylidene cyclopentenedione-based inhibitors have been reported to irreversibly inactivate BoNT/A LC in a biochemical assay by purportedly forming a covalent bond with the enzyme⁴⁶. Finally, the HTS of a natural products library has led to the discovery that lomofungin is a noncompetitive inhibitor of BoNT/A LC ($K_i = 6.7 \pm 0.7 \mu$ M)⁴⁷.

To identify novel small molecule inhibitors of BoNT/A LC, we screened a library of over 70,000 compounds using a fluorescence resonance energy transfer (FRET) assay to detect the inhibition of substrate proteolysis. Structurally novel benzimidazole acrylonitrile hit compound **4** (Figure 1) inhibited BoNT/A LC with low μM -range potency ($\text{IC}_{50} = 7.2 \mu\text{M}$). Modification of the benzimidazole acrylonitrile scaffold represented by compound **4** led to the generation of compound **5** (Figure 1), which displayed improved specificity for BoNT/A LC with respect to other metalloproteases, and provided good SNAP-25 protection in a neuronal assay for BoNT/A intoxication.⁴⁸ Herein, structure-activity relationships, a proposed mechanism of action, and molecular modeling studies for the benzimidazole acrylonitrile series of BoNT/A LC inhibitors are reported.

2. Results and Discussion

2.1. Chemistry

To develop structure-activity relationships (SARs) and potentially improve the potency and specificity of HTS hit compound **4**, the structural modifications illustrated in Figure 2 were performed. Specifically, 1) substituents on the phenyl ring of **4** were modified (see Table 1 for the structures of the modifications) and 2) the phenyl ring of **4** was replaced with a variety of aromatic heterocycles (see Table 2 for the structures of the modifications). Of the derivatives, bisthiophene **5** was the most potent compound *in vitro*. Consequently, this derivative was subjected to further rounds of chemical modification to examine the effects of substituent and core scaffold changes on both *in vitro* potency and specificity (Figure 3) (see Table 4 for the structures of the modifications).

Benzimidazole acrylonitrile compounds **8a**, **8c–k**, **5** and **10a–f** were prepared by condensation of commercially available benzimidazole acetonitrile **6** with a variety of substituted aldehydes (Scheme 1). Specifically, to evaluate the impact of substituents with different chemical and steric properties, the phenyl ring of **4** was substituted with a variety of different substituents (see Table 1 for the structures of the modifications), as well as heteroaromatic rings (see Table 2 for the structures of the modifications).

To develop the SAR for bis-thiophene compound **5**, acrylonitrile derivatives **12a–e** and **14a–d** were synthesized (Schemes 1 and 2, respectively) via acid-catalyzed condensation of aryl acetonitriles **6** and **13** with a variety of substituted aldehydes (*e.g.*, **11** and **9g** in Schemes 1 and 2, respectively) (see Table 4 for the structures of the modifications). Compound **15** was prepared by dimethylation of the benzimidazole ring of compound **5** using methyl iodide (Scheme 3) (see Table 4 for the structure of the modification).

2.2. Biological evaluation

Synthesized derivatives of benzimidazole acrylonitrile **4** were evaluated in a fluorescence resonance energy transfer (FRET)-based recombinant BoNT/A LC assay for inhibitory potency,⁴⁹ and counter screened in an *anthrax* Lethal Factor (LF) assay to provide preliminary indications of selectivity^{49, 50}. Of the synthesized analogs, five provided BoNT/A LC inhibition (Tables 1 and 2). Importantly, no appreciable activity was observed when the derivatives were examined against LF (Tables 1 and 2).

All substituent modifications of structure **4** were detrimental to BoNT/A LC inhibitory potency. For example, removing the 4-OMe group (**8a**), removing the 3-iodo group (**8b**), or replacing it with smaller, and more electronegative halogen atoms (**8c–e**) eliminated inhibitory potency. Moreover, exchanging the 3-iodo substituent for a 3-OMe substituent (**8f**) also eliminated inhibitory potency, while tri-substitutions on the phenyl ring (**8g**, **8h**, **8k**) significantly decreased or diminished activity (*e.g.*, with respect to **4**). Two compounds with 5- or 6-membered aromatic rings appended to the 4-position of the phenyl group (**8i**,

8j) exhibited anti-BoNT/A LC activity, but also with significantly lower potency with respect to **4**. Since modification of the substituents on the phenyl ring failed to improve inhibitory potency, we next examined replacement of the substituted phenyl ring with various aromatic heterocycles including pyridine (**10a**), pyrimidine (**10b**), benzothiophene (**10c**), indoles (**10d–e**), a fused tricyclic ring (**10f**) and bis-thiophene **5**. Inhibition results for these derivatives are shown in Table 2. Only bis-thiophene **5** exhibited significant inhibitory activity against the BoNT/A LC ($IC_{50} = 26 \mu M$) in the FRET-based assay, which was confirmed in a secondary HPLC-based assay ($IC_{50} = 29 \mu M$) (Table 2).

Compounds **4** and **5** were subjected to advanced *in vitro* characterization to determine: 1) enzyme specificity (*e.g.*, in addition to LF inhibition); 2) the possibility of Zn chelation; 3) cellular efficacy; and 4) potential thiol-inactivation (Table 3). With regard to specificity, neither **4** nor **5** inhibited the BoNT serotype B LC.⁴⁸ And while compound **4** was found to modestly inhibit *anthrax* LF ($IC_{50} = 74 \mu M$), compound **5** did not inhibit this enzyme up to concentrations of 100 μM . Additionally, neither compound inhibited human MMP-1, MMP-2 or MMP-9. Overall, the results from the specificity assays clearly demonstrate that compounds **4** and **5** are highly specific for BoNT/A LC.

Examination of the BoNT/A LC inhibitory potencies of **4** and **5** in the presence of 50 μM Zn indicated that neither are metal chelating agents. Neither of these inhibitors displayed a change in inhibitory potency when excess Zn was included in the FRET-based assay (Table 3). Interestingly, compound **4** was inactivated by thiol-containing glutathione and cysteine, while compound **5** showed no significant, non-specific reactivity towards these thiol-containing compounds (Table 3), suggesting that the electrophilicity of the β -carbon of benzimidazole acrylonitrile **5** has been significantly reduced with respect to compound **4**, so that the free sulfhydryl group of glutathione or cysteine is not able to undergo Michael addition to this β -carbon atom.

In chick neuron culture, compound **5** inhibited BoNT/A-mediated SNAP-25 cleavage by 58% at 30 μM concentration, while compound **4** provided approximately 10% inhibition of SNAP-25 cleavage at 30 μM .⁴⁸ During the assay, compound **1** (NSC 240898), a previously reported indole-based BoNT/A LC inhibitor, was used as a positive control, and exhibited a 42% inhibitory activity against BoNT/A-mediated SNAP-25 cleavage at 30 μM .

Based on the high degree of specificity and the SNAP-25 protection provided by **5**, closely related analogs were prepared (see Table 4 for the structures, and Figure 3 for the design strategy). Accordingly, compounds **12a–e**, **14a–d** and **15** were synthesized and their inhibitory efficacies against BoNT/A LC, as well as *anthrax* LF (for preliminary selectivity evaluation) were calculated (Table 4). Compounds containing only one thiophene ring, with various substituents, such as 5-Me (**12a**), 4,5-di-Me (**12b**), or a simple unsubstituted thiophene (**12c**) provided no BoNT/A LC inhibition, while compound **12d**, which possesses a furan ring substituted on the 5-position of the central thiophene, was approximately two-fold less potent than **5** (Table 5). Interestingly, no activity was observed for compound **12e**, which possesses a furan in place of the central thiophene ring in **5**. The bis-thiophene moiety connected directly to the acrylonitrile component is, therefore, highly preferred for anti-BoNT/A LC potency, and the data clearly indicate that even subtle changes to the central thiophene ring have a profoundly negative impact on BoNT/A LC inhibitory potency.

We next kept the bis-thiophene motif intact, and investigated the impact of modification/replacement of the benzimidazole component (Table 4). In particular, replacement of the benzimidazole ring with alternative heterocycles, such as indole (**14a**), benzothiazole (**14b**), benzoxazole (**14c**) and quinoline (**14d**) eliminated inhibitory potency. Moreover, dimethylation of the benzimidazole component (to provide **15**) was also detrimental to

potency. Thus, it appears that the benzimidazole core is necessary for BoNT/A LC inhibition with this chemotype.

2.3. Mechanism of action

Benzimidazole acrylonitriles **4** and **5** demonstrated noncompetitive kinetics with respect to the substrate (17-mer SNAPtide), which suggested that the inhibitors are not binding in the BoNT/A LC active site.⁴⁸ Therefore, enzyme/inhibitor “rescue studies” were performed to further characterize the mechanism of action of **4** and **5** (Table 5). Inactivation was detected when BoNT/A LC was incubated with the benzimidazole acrylonitrile inhibitors and subsequently subjected to dialysis. Specifically, we found that the inhibitors were bound to the protein fraction, and could only be partially recovered. However, this inactivation was prevented when the BoNT/A LC was simultaneously incubated in the presence of a benzimidazole acrylonitrile inhibitor and known competitive inhibitor **2** (and then subjected to dialysis); benzimidazole acrylonitrile could be recovered during this dialysis experiment. Hence, this experiment indicated that even though benzimidazole acrylonitriles are not active site inhibitors, they may bind to a site close to the active site, and that the active site inhibitor may interfere with the binding of the benzimidazole acrylonitrile inhibitors by partially blocking their enzyme interaction site. Further analysis of the mechanism of action has revealed that compounds **4** and **5** inhibit BoNT/A LC in a time-dependent manner: when compound **5** was pre-incubated with enzyme for 90 minutes (assay time was 40 minutes), the IC₅₀ value decreased from 26 μM (no preincubation; FRET assay) to 17 μM (FRET assay), suggesting that this compound is a time-dependent inhibitor. The specificity constant k_{inact}/K_i values for compounds **4** and **5** were measured as 979 and 326 M⁻¹s⁻¹, respectively (Figures 4 and 5)^{46, 51}. The time-dependent inactivation of BoNT/A LC by **4** and **5** suggests that covalent modification of the target enzyme may occur in their mechanism of action.

2.4. Molecular modeling

To identify a nucleophilic amino acid that could be responsible for the generation of a covalent adduct, we first examined the amino acid sequence of BoNT/A LC (425 AAs, PDB reference code 3BOK_A) and identified two cysteine residues located at positions 134 and 165 (Figure 6). Cysteine is the most intrinsically nucleophilic amino acid residue in proteins, and in addition to its role in catalysis, it is subject to posttranslational chemical modifications that are related to its nucleophilicity⁵². Examination of the crystal structure (PDB reference code: 2G7N) of BoNT/A LC indicates that positively charged Arg231 is located within 5 Å of Cys165, while Cys165 is negatively charged and coordinated with two silver cations in the crystal structure. No positively charged amino acid residues were observed within 5 Å of Cys134. Cys165 is located approximately 8 Å from the enzyme catalytic Zn²⁺ ion, while Cys134 is located on a β-sheet structure that is in the bottom bay area opposite to the entrance to the β-exosite⁵³. Consequently, we hypothesized that benzimidazole acrylonitrile inhibitors could inactivate BoNT/A LC by forming a covalent bond with one of these two cysteine residues.

Mechanistically, two steps are generally proposed for covalent bond formation. Initially, the inhibitor binds to the target enzyme to form a non-covalent Michaelis complex (EI*), which then proceeds through a second step to yield the covalent adduct (EI)⁵⁴. With this knowledge, a computational modeling study was performed to identify which cysteine residue might be involved in the covalent modification process. Compound **5** was first non-covalently docked into sites in the proximity of both Cys134 and Cys165, and it displayed greater binding affinity for the Cys165 site than for the Cys134 site. Moreover, when compound **5** was docked non-covalently near the Cys165 residue (Figure 7), thereby mimicking the Michaelis complex (EI*), its electrophilic double bond was in a favorable orientation that would accommodate nucleophilic attack by the Cys165 sulfhydryl group.

The S-C_β distance is about 4.3 Å, which renders the nucleophilic Michael addition reaction plausible, without the need to overcome a high energy barrier. Interestingly, the guanidine group of Arg177 forms hydrogen bonds with one of the benzimidazole nitrogen atoms and the nitrile group of **5**, which further stabilizes the noncovalent Michaelis complex. Conversely, in the best docking mode for compound **5** in the Cys134 site, the S-C_β distance is about 9.1 Å, and the geometry of compound **5** is not favorable for covalent bond formation (Figure 8). We have demonstrated earlier that compound **5** does not react with free cysteine due to the reduced electrophilicity of the β-carbon. However, the pKa value of most protein cysteine thiols is between 8–9,⁵⁵ while the Cys165 residue exists as a thiolate anion at neutral pH and is in close proximity to the positively charged Arg231 residue. The lower pKa value of the Cys165 allows it to be sufficiently nucleophilic to interact with compound **5** to form a covalent bond. The proximity of the nucleophile to the electrophile in the bound structure offers an entropic advantage to subsequent covalent bond formation. Taking this information into account, *we propose that Cys165 is the preferred nucleophilic amino acid for covalent modification of compound 5, and that a Michael addition occurs between the sulfhydryl group of Cys165 and the acrylonitrile functionality of compound 5 to produce persistent inactivation of BoNT/A LC* (Figure 9). We have termed the Cys165 site as the T-exosite, to supplement the known substrate SNAP-25 α- and β-exosites⁵³.

In support of our hypothesis, the inactivation of other protein targets via the covalent binding of an inhibitor to a specific, noncatalytic cysteine residue has been demonstrated. Examples include several kinase inhibitors⁵⁶ and HCV protease inhibitors⁵⁷. Interestingly, we noticed that nucleophilic cysteine residues involved in the covalent enzyme inactivation of other enzymes are generally located near their active sites or substrate binding sites. For example, a noncatalytic Cys797 is near the ATP binding site in Epidermal Growth Factor Receptor (EGFR) kinase⁵⁸, and a Cys159 is close to the substrate binding site of HCV NS3/4a protease⁵⁷. Both of these sites have been used to develop inhibitors that form a covalent bond with their respective target enzymes^{56, 57}. Currently, we are unable to generate X-ray co-crystal structures of compound **5** with BoNT/A LC due to the low aqueous solubility of the compound, and a preliminary liquid chromatography-mass spectrometry (LC-MS) experiment was performed in an attempt to detect a covalent adduct, which was also unsuccessful.

With regard to compound **5**, it is also important to note that the nucleophilic Michael addition occurring between the Cys165 sulfhydryl group and the acrylonitrile double bond generates two new chiral centers in the inhibitor structure. Consequently, four covalently-bound diastereomers are possible. Therefore, we modeled all four possible diastereomeric covalent adducts, and of the four, the covalent (2S, 3R)-**5**:BoNT/A LC adduct demonstrated the lowest binding energy compared to the other three adducts. The modeled structure of the (2S, 3R)-**5**:BoNT/A LC adduct is shown in Figure 10. The orientation of the inhibitor in this structure is similar to its orientation in the non-covalent Michaelis-like complex (Figure 7). The inhibitor benzimidazole ring is positioned near the catalytic site, and the bis-thiophene moiety is bound along the β-sheet structure containing Cys165. Interestingly, the nitrile group maintains its hydrogen bonding interaction with Arg177 (compare Figure 7 and Figure 10), which further enhances binding affinity. Finally, it is also important to note that, even though the actual function of Cys 165 is unknown, covalent modification of Cys 165 would prevent the BoNT/LC mediated SNAP-25 cleavage.

3. Conclusion

A novel benzimidazole acrylonitrile BoNT/A LC inhibitor chemotype was identified during the HTS of a library containing 70,000 small molecules. Modification of hit compound **4** led to the generation of compound **5**, which displays a high degree of specificity for BoNT/A

LC with respect to other metalloproteases, and demonstrates SNAP-25 protection in neurons during BoNT/A challenge. Structure-activity relationship studies were performed to define the chemical features of compound **5** that are important for BoNT/A LC inhibitory potency. In summary, we have discovered a highly specific, time-dependent inhibitor that inactivates BoNT/A LC through the proposed covalent modification of a non-catalytic cysteine residue in a previously unidentified substrate binding site. Our ultimate goal for this class of inhibitor is to examine representative compounds in *in vivo* models of BoNT/A intoxication.

4. Experimental section

4.1 General procedures

All commercially obtained solvents and reagents were used as received. Melting points were determined in open capillary tubes with an EZ-Melt (Stanford Research Systems) apparatus and are uncorrected. ^1H NMR spectra were determined on a Bruker 300 MHz instrument. Chemical shifts are given in δ values referenced to the internal standard tetramethylsilane. LC-MS analyses were performed by CreaGen Biosciences, Inc. (Woburn, MA) using a Shimadzu LC-10 AD VP HPLC and a Waters micromass quattro ultima triple-quad MS. All of the compounds tested *in vitro* possessed >95% purity based on LC-MS analyses. Only one regioisomer was observed for the benzimidazole acrylonitrile compounds based on the ^1H NMR and LC-MS.

4.2. The general synthesis of acrylonitrile compounds

Aryl acetonitrile (3.2 mmol, 1.0 eq.), aldehyde (3.2 mmol, 1.0 eq.), and ammonium acetate (9.5 mmol, eq.) were mixed in glacial acetic acid (10 mL) and heated at reflux for 2 h. Following, the reaction mixture was cooled to room temperature. The precipitate that formed was collected by filtration, washed with water, followed by a small volume of methanol, and dried in a vacuum oven at 50 °C for 18 h.

2-(1-Cyano-2-phenylvinyl)benzimidazole (8a)—Light brown powder, $R_f = 0.35$ (1:4 EtOAc/hexane), mp = 259–260 °C; ^1H NMR (300 MHz, DMSO- d_6) δ 13.09 (s, 1H), 8.34 (s, 1H), 8.28 (s, 1H), 7.96 (dd, $J = 8.1, 12$ Hz, 2H), 7.71 (d, $J = 7.2$ Hz, 1H), 7.58 (d, $J = 5.7$ Hz, 1H), 7.41 (t, $J = 7.8$ Hz, 1H), 7.3–7.24 (m, 2H). LC-MS (+ESI): m/z 372.07 (M+1) $^+$.

2-(1-Cyano-2-phenylvinyl)benzimidazole (8b)—Yellow powder, $R_f = 0.16$ (1:4 EtOAc/hexane), mp = 223–224 °C; ^1H NMR (300 MHz, DMSO- d_6) δ 12.98 (br, s, 1H), 8.28 (s, 1H), 8.01 (d, $J = 8.1, 2$ Hz), 7.64 (br, s, 1H), 7.59 (br, s, 1H), 7.25 (d, $J = 7.8$ Hz, 1H), 7.17 (d, $J = 8.1$ Hz, 2H), 3.87 (s, 3H). LC-MS (+ESI): m/z 276.2 (M+1) $^+$.

2-(1H-Benzo[d]imidazol-2-yl)-3-(4-methoxy-3-bromophenyl)acrylonitrile (8c)—Yellow solid, $R_f = 0.65$ (1:1 EtOAc/hexane), mp = 253–254 °C; ^1H NMR (300 MHz, DMSO- d_6) δ 12.99 (br, s, 1H), 8.28 (d, $J = 2.4$ Hz, 1H), 8.26 (s, 1H), 8.00 (dd, $J = 2.1, 8.9$ Hz, 1H), 7.66 (br, s, 1H), 7.58 (br, s, 1H), 7.35 (d, $J = 8.7$ Hz, 1H), 7.26 (br, d, $J = 4.8$ Hz, 2H), 3.97 (s, 3H). LC-MS (+ESI): m/z 354.1 (M+1) $^+$.

(1H-Benzo[d]imidazol-2-yl)-3-(3-chloro-4-methoxyphenyl)acrylonitrile (8d)—Pale yellow solid, $R_f = 0.71$ (1:1 EtOAc/hexane), mp = 250–251 °C; ^1H NMR (300 MHz, DMSO- d_6) δ 13.0 (s, 1H), 8.26 (s, 1H), 8.12 (d, $J = 2.4$ Hz, 1H), 7.96 (dd, $J = 2.1, 8.7$ Hz, 1H), 7.69 (d, $J = 7.2$ Hz, 1H), 7.56 (d, $J = 7.2$ Hz, 1H), 7.38 (d, $J = 8.7$ Hz, 1H), 7.31–7.21 (m, 2H), 3.98 (s, 3H). LC-MS (+ESI): m/z 310.17 (M+1) $^+$.

2-(1H-Benzo[d]imidazol-2-yl)-3-(3-fluoro-4-methoxyphenyl)acrylonitrile (8e)—Light yellow solid, $R_f = 0.50$ (1:1 EtOAc/hexane), mp = 271–272 °C; ^1H NMR (300 MHz,

DMSO-*d*₆) δ 13.01 (s, 1H), 8.27 (s, 1H), 7.92 (dd, *J* = 2.1, 15 Hz, 1H), 7.81 (d, *J* = 8.4 Hz, 1H), 7.62 (s, br, 2H), 7.39 (t, *J* = 8.7 Hz, 1H), 7.26 (dd, *J* = 3, 6 Hz, 2H), 3.96 (s, 3H). LC-MS (+ESI): *m/z* 294.17 (M+1)⁺.

2-(1*H*-Benzo[d]imidazol-2-yl)-3-(3,4-dimethoxyphenyl)acrylonitrile (8f)—Yellow solid, *R*_f = 0.54 (1:1 EtOAc/hexane), mp = 184–185 °C; ¹H NMR (300 MHz, DMSO-*d*₆) δ 12.98 (br, s, 1H), 8.27 (s, 1H), 7.74 (d, *J* = 2.1 Hz, 1H), 7.62 (br, s, 1H), 7.58 (dd, *J* = 2.1, 6.0 Hz, 2H), 7.62–7.23 (m, 2H), 7.19 (d, *J* = 8.7 Hz, 1H), 3.88 (s, 3H), 3.86 (s, 3H). LC-MS (+ESI): *m/z* 306.23 (M+1)⁺.

2-[1-Cyano-2-(3-chloro-5-methoxy-4-hydroxyphenyl)vinyl]benzimidazole (8g)—Light orange solid, *R*_f = 0.55 (80:18:2 CHCl₃/CH₃OH/CH₃NH₂), mp = 286–287 °C; ¹H NMR (300 MHz, DMSO-*d*₆) δ 12.99 (br, s, 1H), 10.65 (br, s, 1H), 8.22 (s, 1H), 7.67 (s, 3H), 7.57 (br, s, 1H), 7.26 (d, *J* = 5.1 Hz, 2H), 3.93 (s, 3H). LC-MS (+ESI): *m/z* 326.18 (M+1)⁺.

2-[1-Cyano-2-(3-bromo-5-methoxy-4-hydroxyphenyl)vinyl]benzimidazole (8h)—Light orange solid, *R*_f = 0.61 (80:18:2 CHCl₃/CH₃OH/CH₃NH₂), mp = 268–269 °C; ¹H NMR (300 MHz, DMSO-*d*₆) δ 12.98 (br, s, 1H), 10.69 (br, s, 1H), 8.23 (s, 1H), 7.796 (d, *J* = 2.1 Hz, 1H), 7.706 (d, *J* = 1.8 Hz, 1H), 7.67 (br, s, 1H), 7.57 (br, s, 1H), 7.3–7.2 (m, 2H), 3.93 (s, 3H). LC-MS (+ESI): *m/z* 372.16 (M+1)⁺.

2-(1*H*-Benzo[d]imidazol-2-yl)-3-(biphenyl-4-yl)acrylonitrile (8i)—Yellow solid, *R*_f = 0.33 (1:4 EtOAc/hexane), mp = 267–268 °C; ¹H NMR (300 MHz, DMSO-*d*₆) δ 13.11 (s, 1H), 8.39 (s, 1H), 8.11 (d, *J* = 8.4 Hz, 2H), 7.94 (d, *J* = 8.4 Hz, 2H), 7.80 (dd, *J* = 1.5, 7.7 Hz, 2H), 7.73–7.69 (m, 1H), 7.59–7.42 (m, 4H), 7.33–7.23 (m, 2H). LC-MS (+ESI): *m/z* 322.29 (M+1)⁺.

3-(4-(1*H*-Imidazol-1-yl)phenyl)-2-(1*H*-benzo[d]imidazol-2-yl)acrylonitrile (8j)—Light yellow solid. *R*_f = 0.67 (1:1 EtOAc/hexane), mp = 267–268 °C; ¹H NMR (300 MHz, DMSO-*d*₆) δ 13.06 (br, s, 1H), 8.46 (s, 1H), 8.39 (s, 1H), 8.14 (d, *J* = 8.7 Hz, 2H), 7.95 (s, 1H), 7.92–7.91 (m, 2H), 7.65 (br, s, 2H), 7.29–7.26 (m, 2H), 7.18 (s, 1H). LC-MS (+ESI): *m/z* 312.26 (M+1)⁺.

2-(1*H*-Benzo[d]imidazol-2-yl)-3-(3-hydroxy-4,5-dimethoxyphenyl)acrylonitrile (8k)—Yellow powder, *R*_f = 0.81 (80:18:2 CHCl₃/CH₃OH/CH₃NH₂), mp = 260–261 °C; ¹H NMR (300 MHz, DMSO-*d*₆) δ 12.98 (br s, 1H), 9.79 (br s, 1H), 8.19 (s, 1H), 7.63 (br s, 2H), 7.28–7.25 (m, 2H), 7.22 (d, 2H), 3.86 (s, 3H), 3.79 (s, 3H). LCMS (+ESI): *m/z* 322.18 (M+1)⁺.

2-[1-Cyano-2-(2-chloro-5-phenylpyridin-3-yl)vinyl]-benzimidazole (10a)—Bright yellow solid, *R*_f = 0.82 (1:1 EtOAc/hexane), mp = 270–271 °C; ¹H NMR (300 MHz, DMSO-*d*₆) δ 13.43 (br, 1H), 8.88 (dd, *J* = 2.4, 12.6 Hz, 2H), 8.49 (s, 1H), 7.83 (d, *J* = 7.2 Hz, 2H), 7.68 (br, 2H), 7.61–7.49 (m, 3H). LC-MS (+ESI): *m/z* 355.2 (M-1)⁻.

2-[1-Cyano-2-(2,4-dichloropyrimidin-3-yl)vinyl]-benzimidazole (10b)—Light orange solid, *R*_f = 0.01 (1:1 EtOAc/hexane), mp >300 °C; ¹H NMR (300 MHz, DMSO-*d*₆) δ 13.42 (br, 1H), 8.85 (d, *J* = 8.1 Hz, 1H), 8.69 (s, 1H), 8.56 (s, 1H), 7.94 (d, *J* = 7.8 Hz, 1H), 7.62 (t, *J* = 7.2 Hz, 1H), 7.51 (t, *J* = 7.5 Hz, 1H).

2-(1*H*-Benzo[d]imidazol-2-yl)-3-(3-methylbenzo[b]thiophen-2-yl)acrylonitrile (10c)—Light orange solid, *R*_f = 0.78 (1:1 EtOAc/hexane), mp = 267–268 °C; ¹H NMR (300 MHz, DMSO-*d*₆) δ 13.19 (br, 1H), 8.64 (s, 1H), 8.11 (dd, *J* = 1.2, 6.7 Hz, 1H), 7.99 (dd, *J* =

2.1, 6.9 Hz, 1H), 7.71 (br, 1H), 7.59–7.49 (m, 3H), 7.30–7.25 (m, 2H), 2.74 (s, 3H). LC-MS (+ESI): *m/z* 316.48 (M+1)⁺.

1*H*-Benzo[d]imidazol-2-yl)-3-(5-bromo-1*H*-indol-3-yl)acrylonitrile (10d)—Bright yellow solid, *R_f* = 0.61 (1:1 EtOAc/hexane), mp >300 °C; ¹H NMR (300 MHz, DMSO-*d*₆) δ 12.86 (br, s, 1H), 12.42 (br, s, 1H), 8.59 (s, 1H), 8.52 (s, 1H), 8.21 (s, 1H), 7.66 (br, s, 1H), 7.56 (d, *J* = 8.4 Hz, 2H), 7.42 (dd, *J* = 1.8, 8.7 Hz, 1H), 7.24 (br, s, 2H). LC-MS (+ESI): *m/z* 363.14 (M+1)⁺.

2-(1*H*-Benzo[d]imidazol-2-yl)-3-(4-nitro-1*H*-indol-3-yl)acrylonitrile (10e)—Orange yellow solid, *R_f* = 0.20 (1:1 EtOAc/hexane), mp >300 °C; ¹H NMR (300 MHz, DMSO-*d*₆) δ 12.93 (br, s, 2H), 8.69 (d, *J* = 8.1 Hz, 2H), 8.05 (dd, *J* = 8.1, 12.3 Hz, 2H), 7.64 (br, s, 2H), 7.45 (t, *J* = 15.9 Hz, 1H), 7.28–7.25 (m, 2H). LC-MS (+ESI): *m/z* 330.2 (M+1)⁺.

2-(1*H*-Benzo[d]imidazol-2-yl)-3-(1*H*-benzo[g]indol-3-yl)acrylonitrile (10f)—Yellow solid, *R_f* = 0.77 (1:1 EtOAc/hexane), mp >300 °C; ¹H NMR (300 MHz, DMSO-*d*₆) δ 13.04 (br, s, 2H), 8.75 (s, 1H), 8.54 (s, 1H), 8.48 (d, *J* = 8.1 Hz, 1H), 8.13 (d, *J* = 8.7 Hz, 1H), 8.05 (d, *J* = 8.1 Hz, 1H), 7.79 (d, *J* = 9 Hz, 1H), 7.69–7.64 (m, 3H), 7.54 (t, *J* = 7.2 Hz, 1H), 7.27–7.24 (m, 2H). LC-MS (+ESI): *m/z* 335.3 (M+1)⁺.

3-(2,2'-Bithiophen-5-yl)-2-(1*H*-benzo[d]imidazol-2-yl)acrylonitrile (5)—Orange brown solid, *R_f* = 0.69 (1:1 EtOAc/hexane), mp = 271–272 °C; ¹H NMR (300 MHz, DMSO-*d*₆) δ 13.00 (s, 1H), 8.51 (s, 1H), 7.79 (d, *J* = 3.9 Hz, 1H), 7.71–7.66 (m, 2H), 7.58 (dd, *J* = 1.2, 3.0 Hz, 1H), 7.54 (d, *J* = 4.2 Hz, 2H), 7.28–7.23 (m, 2H), 7.21–7.18 (m, 1H). LC-MS (+ESI): *m/z* 334.15 (M+1)⁺.

2-(1*H*-Benzo[d]imidazol-2-yl)-3-(5-methylthiophen-2-yl)acrylonitrile (12a)—Bright orange solid, *R_f* = 0.38 (1:4 EtOAc/hexane), mp = 279–280 °C; ¹H NMR (300 MHz, DMSO-*d*₆) δ 12.94 (s, 1H), 8.45 (s, 1H), 7.66 (d, *J* = 3.6 Hz, 2H), 7.54 (br, 1H), 7.23 (d, *J* = 4.8 Hz, 2H), 7.06 (dd, *J* = 0.9, 3.6 Hz, 1H), 2.59 (s, 3H). LC-MS (+ESI): *m/z* 266.44 (M+1)⁺.

2-(1*H*-Benzo[d]imidazol-2-yl)-3-(4,5-dimethylthiophen-2-yl)acrylonitrile (12b)—Brown yellow solid, *R_f* = 0.44 (1:4 EtOAc/hexane), mp = 291–292 °C; ¹H NMR (300 MHz, DMSO-*d*₆) δ 12.92 (s, 1H), 8.36 (s, 1H), 7.59 (br, 1H), 7.54 (s, 1H), 7.23 (dd, *J* = 2.7, 6.0 Hz, 2H), 2.43 (s, 3H), 2.16 (s, 3H). LC-MS (+ESI): *m/z* 280.5 (M+1)⁺.

2-(1*H*-Benzo[d]imidazol-2-yl)-3-(thiophen-2-yl)acrylonitrile (12c)—Bright yellow solid, *R_f* = 0.38 (1:4 EtOAc/hexane), mp = 222–223 °C; ¹H NMR (300 MHz, DMSO-*d*₆) δ 13.02 (br, 1H), 8.56 (s, 1H), 8.07 (d, *J* = 4.8 Hz, 1H), 7.86 (d, *J* = 3.6 Hz, 1H), 7.68 (d, *J* = 7.8 Hz, 1H), 7.55 (d, *J* = 7.8 Hz, 1H), 7.35 (dd, *J* = 3.6, 4.9 Hz, 1H), 7.30–7.21 (m, 2H). LC-MS (+ESI): *m/z* 252.3 (M+1)⁺.

2-(1*H*-Benzo[d]imidazol-2-yl)-3-(5-(furan-2-yl)thiophen-2-yl)acrylonitrile (12d)—Dark brown solid, *R_f* = 0.79 (1:1 EtOAc/hexane), mp = 273–274 °C; ¹H NMR (300 MHz, DMSO-*d*₆) δ 12.99 (br, 1H), 8.52 (s, 1H), 7.87 (d, *J* = 1.8 Hz, 1H), 7.81 (d, *J* = 4.5 Hz, 1H), 7.66 (br, 1H), 7.58–7.53 (m, 2H), 7.26–7.24 (m, 2H), 7.11 (d, *J* = 3.6 Hz, 1H), 6.70 (dd, *J* = 1.8, 4.5 Hz, 1H). LC-MS (+ESI): *m/z* 318.44 (M+1)⁺.

2-(1*H*-Benzo[d]imidazol-2-yl)-3-(5-(thiophen-2-yl)furan-2-yl)acrylonitrile hemiacetate (12e)—Orange solid, *R_f* = 0.59 (1:2 EtOAc/hexane), mp = 243–244 °C; ¹H NMR (300 MHz, DMSO-*d*₆) δ 13.0 (s, 1H), 11.98 (s, 0.5 H), 8.14 (s, 1H), 7.76 (dd, *J* = 0.9,

4.9 Hz, 1H), 7.67(dd, $J = 1.2, 3.6$ Hz, 2H), 7.53 (d, $J = 7.5$ Hz, 1H), 7.42 (d, $J = 3.6$ Hz, 1H), 7.26–7.22 (m, 3H), 7.17 (d, $J = 3.6$ Hz, 1H), 1.92 (s, 1.5 H). LC-MS (+ESI): m/z 318.44 (M+1)⁺.

3-(2,2'-Bithiophen-5-yl)-2-(1*H*-indol-2-yl)acrylonitrile (14a)—Orange solid, $R_f = 0.38$ (1:4 EtOAc/hexane), mp = 245–246 °C; ¹H NMR (300 MHz, DMSO-*d*₆) δ 11.72 (br, s, 1H), 8.08 (s, 1H), 7.65 (dd, $J = 0.9, 5.1$ Hz, 1H), 7.59–7.57 (m, 2H), 7.51 (dd, $J = 0.9, 3.6$ Hz, 1H), 7.47 (d, $J = 3.9$ Hz, 1H), 7.41 (dd, $J = 0.3, 9$ Hz, 1H), 7.22–7.15 (m, 2H), 7.05 (ddd, $J = 0.9, 8.1, 15$ Hz, 1H), 6.77 (s, 1H). LC/MS (+ESI): m/z 333.3 (M+1)⁺.

3-(2,2'-Bithiophen-5-yl)-2-(benzo[d]thiazol-2-yl)acrylonitrile (14b)—Red solid, $R_f = 0.60$ (1:4 EtOAc/hexane), mp = 188–189 °C; ¹H NMR (300 MHz, DMSO-*d*₆) δ 8.61 (s, 1H), 8.16 (dd, $J = 0.6, 7.9$ Hz, 1H), 8.05 (dd, $J = 0.6, 7.8$ Hz, 1H), 7.99 (d, $J = 4.5$ Hz, 1H), 7.73 (dd, $J = 0.9, 5.1$ Hz, 1H), 7.60 (dd, $J = 1.2, 3.8$ Hz, 1H), 7.57 (d, $J = 3.9$ Hz, 1H), 7.53 (dd, $J = 1.2, 9.6$ Hz, 1H), 7.48 (dd, $J = 0.9, 7.4$ Hz, 1H), 7.19 (dd, $J = 3.9, 5.1$ Hz, 1H). LC-MS (+ESI): m/z 351.25 (M+1)⁺.

3-(2,2'-Bithiophen-5-yl)-2-(benzo[d]oxazol-2-yl)acrylonitrile (14c)—Dark red solid, $R_f = 0.84$ (1:2 EtOAc/hexane), mp = 192–193 °C; ¹H NMR (300 MHz, DMSO-*d*₆) δ 8.67 (s, 1H), 8.0 (d, $J = 3.9$ Hz, 1H), 7.80–7.69 (m, 3H), 7.66 (dd, $J = 3.2, 0.9$ Hz, 1H), 7.56 (d, $J = 3.9$ Hz, 1H), 7.47–7.39 (m, 2H), 7.18 (dd, $J = 4.5, 1.2$ Hz, 1H). LC-MS (+ESI): m/z 335.43 (M+1)⁺.

3-(2,2'-Bithiophen-5-yl)-2-(quinolin-2-yl)acrylonitrile (14d)—Brown solid, $R_f = 0.87$ (1:4 EtOAc/hexane), mp = 174–175 °C; ¹H NMR (300 MHz, DMSO-*d*₆) δ 8.82 (s, 1H), 8.49 (d, $J = 8.7$ Hz, 1H), 8.07–8.0 (m, 3H), 7.90 (d, $J = 3.9$ Hz, 1H), 7.83 (ddd, $J = 1.5, 7.2, 15.6$ Hz, 1H), 7.69 (dd, $J = 1.2, 5.1$ Hz, 1H), 7.64 (ddd, $J = 1.2, 8.1, 15.0$ Hz, 1H), 7.58 (dd, $J = 1.2, 3.6$ Hz, 1H), 7.55 (d, $J = 3.9$ Hz, 1H), 7.19 (dd, $J = 3.6, 4.9$ Hz, 1H). LC-MS (+ESI): m/z 345.5 (M+1)⁺.

2-(2-(2,2'-Bithiophen-5-yl)-1-cyanovinyl)-1,3-dimethyl-1*H*-benzo[d]imidazol-3-ium iodide (15)—A mixture of 2-[1-cyano-2-(2,2'-bithiophen-5-yl)vinyl]benzimidazole (150 mg, 0.45 mmol) and NaH (60% in oil) (270 mg, 0.67 mmol) was stirred in DMF (5 mL) at 43 °C for 15 min. Methyl iodide (960 mg, 42 μL, 0.67 mol) was added and the reaction mixture was stirred for 24 h. The solution was poured into excess water, in which produced a sticky brown precipitate. EtOAc was added and the mixture was stirred for 1 h. The precipitate turned into a brick red solid, which was collected by filtration, washed with water and dried at 50 °C under vacuum overnight to give the desired product (70 mg, 32%), $R_f = 0.73$ (1:5 MeOH/CH₂Cl₂), mp = 232–233 °C; ¹H NMR (300 MHz, DMSO-*d*₆) δ 8.49 (s, 1H), 8.14 (d, $J = 3.3$ Hz, 1H), 8.12 (d, $J = 3.3$ Hz, 1H), 8.03 (d, $J = 4.2$ Hz, 1H), 7.81 (d, $J = 5.1$ Hz, 1H), 7.78 (d, $J = 3.3$ Hz, 1H), 7.76 (d, $J = 3.3$ Hz, 1H), 7.72 (d, $J = 3.6$ Hz, 1H), 7.69 (d, $J = 3.9$ Hz, 1H), 7.25 (dd, $J = 1.2, 4.5$ Hz, 1H), 4.13 (s, 6H). LC-MS (+ESI): m/z 362.3 (M)⁺.

4.3. BoNT/A LC FRET-based assay

The fluorescence resonance energy transfer (FRET)-based assay used in these studies has been described previously^{7, 8}. Briefly, 20 μM SNAP-25 substrate (AA 187–203) of sequence SNRTRIDEAN[DnpK]RA[daciaC]RML (Peptides International, Kentucky) was incubated at 37 °C for 40 min in the presence of 2 nM BoNT/A LC (List Biologicals, California). The fluorescence of the cleaved substrate was measured at 485 nm following excitation at 398 nm in a Victor 2 (Perkin Elmer, Waltham, MA) plate reader. IC₅₀ values were calculated as the concentration of compound that produced 50% inhibition in the assay.

4.4. BoNT/A LC HPLC-based assay

The BoNT/A LC HPLC-based assay to quantitate inhibition is a modified version of a published protocol⁴⁹. Incubation conditions were the same as for the FRET-based assay, except that the enzyme concentration was 6 nM and the substrate (17-mer SNAPtide) concentration was 60 μ M. The samples were analyzed by reverse-phase HPLC (Gilson, Wisconsin) using a C18 column (Grace Alltima, UK). The effluent was monitored at 365 nm and the resultant peaks quantified by integration utilizing Gilson Trilution® software.

4.5. Anthracis Lethal Factor (LF) assay

A LF FRET-based assay was performed using peptide substrate (MCA-KKVYPYPME[dnp]K amide), and 5.55 nM BaLF (List Biological, California), and incubating at 37 °C for 30 min as described previously^{49, 50}.

4.6. Enzyme inhibitor inactivation studies

BoNT/A LC was incubated with select concentrations of inhibitor at various time points. At the end of the incubation period, remaining enzyme activity was assessed using the BoNT/A LC FRET-based assay (described above). Results were plotted and $K_{obs}/[I]$ were determined utilizing a method by Adam *et al*⁵¹.

4.7. Enzyme/Inhibitor “rescue” studies

BoNT/A LC was co-incubated with DMSO equivalent (control) or inhibitor at 37 °C for 90 minutes. The experimental samples (500 μ L) were then loaded into dialysis cassettes (Pierce 66330 cassettes 3,500 molecular weight cutoff) and dialyzed against 1L of 20 mM HEPES pH 7.4, 10 % Glycerol, and 0.05 % Tween-20 for 20–24 h at 2–8 °C. The experimental samples were then assessed for remaining activity using the standard FRET-based assay (indicated above). The enzyme-inhibitor activity that remained was compared to either the DMSO equivalent or the DMSO equivalent/50 μ M compound **2** (acetic acid salt form) for the competitive inhibitor protection studies.

4.8. Molecular modeling

Docking calculations were performed using Schrödinger Glide 5.0 software (Schrödinger, New York). The covalent adducts were constructed using the ‘best’ docking mode and the energy of the inhibitor-enzyme adduct was fully minimized until RMSD < 0.3 Å.

Acknowledgments

This work was supported by the National Institutes of Health/National Institute of Allergy and Infectious Diseases (5U01AI070430). The content of this publication does not necessarily reflect the views or policies of the Department of Health and Human Services. The authors thank Dr. James C. Burnett for helpful discussions and Dr. Donald T. Moir for assistance with the kinetic analyses. The authors thank CreaGen Biosciences, Inc., for the preparation of starting material, e.g., 2-(1*H*-indol-2-yl)acetonitrile (**6**) and for the scale-up of compound **14a**.

References and notes

1. Arnon SS, Schechter R, Inglesby TV, Henderson DA, Bartlett JG, Ascher MS, Eitzen E, Fine AD, Hauer J, Layton M, Lillibridge S, Osterholm MT, O'Toole T, Parker G, Perl TM, Russell PK, Swerdlow DL, Tonat K. Botulinum toxin as a biological weapon: medical and public health management. *Jama*. 2001; 285:1059–1070. [PubMed: 11209178]
2. Paddle BM. Therapy and prophylaxis of inhaled biological toxins. *J. Appl. Toxicol.* 2003; 23:139–170. [PubMed: 12794937]
3. Burnett JC, Henchal EA, Schmaljohn AL, Bavari S. The evolving field of biodefense: therapeutic developments and diagnostics. *Nat. Rev. Drug Discov.* 2005; 4:281–297. [PubMed: 15803193]

4. Burnett JC, Schmidt JJ, McGrath CF, Nguyen TL, Hermone AR, Panchal RG, Vennerstrom JL, Kodukula K, Zaharevitz DW, Gussio R, Bavari S. Conformational sampling of the botulinum neurotoxin serotype A light chain: implications for inhibitor binding. *Bioorg. Med. Chem.* 2005; 13:333–341. [PubMed: 15598556]
5. Josko D. Botulin toxin: a weapon in terrorism. *Clin. Lab. Sci.* 2004; 17:30–34. [PubMed: 15011978]
6. Clarke SC. Bacteria as potential tools in bioterrorism, with an emphasis on bacterial toxins. *Br. J. Biomed. Sci.* 2005; 62:40–46. [PubMed: 15816214]
7. Hicks RP, Hartell MG, Nichols DA, Bhattacharjee AK, van Hamont JE, Skillman DR. The medicinal chemistry of botulinum, ricin and anthrax toxins. *Curr. Med. Chem.* 2005; 12:667–690. [PubMed: 15790305]
8. Shukla HD, Sharma SK. Clostridium botulinum: a bug with beauty and weapon. *Crit. Rev. Microbiol.* 2005; 31:11–18. [PubMed: 15839401]
9. Comella CL, Pullman SL. Botulinum toxins in neurological disease. *Muscle Nerve.* 2004; 29:628–644. [PubMed: 15116366]
10. Glogau RG. Review of the use of botulinum toxin for hyperhidrosis and cosmetic purposes. *Clin. J. Pain.* 2002; 18:S191–S197. [PubMed: 12569968]
11. Marks JD. Medical aspects of biologic toxins. *Anesthesiol. Clin. North America.* 2004; 22:509–532. vii.. [PubMed: 15325716]
12. Montecucco C, Molgo J. Botulin neurotoxins: revival of an old killer. *Curr. Opin. Pharmacol.* 2005; 5:274–279. [PubMed: 15907915]
13. Bhidayasiri R, Truong DD. Expanding use of botulinum toxin. *J. Neurol. Sci.* 2005; 235:1–9. [PubMed: 15990116]
14. Bigalke H, Rummel A. Medical aspects of toxin weapons. *Toxicology.* 2005; 214:210–220. [PubMed: 16087285]
15. Foster KA. A new wrinkle on pain relief: re-engineering clostridial neurotoxins for analgesics. *Drug Discov. Today.* 2005; 10:563–569. [PubMed: 15837599]
16. Cote TR, Mohan AK, Polder JA, Walton MK, Braun MM. Botulinum toxin type A injections: adverse events reported to the US Food and Drug Administration in therapeutic and cosmetic cases. *J. Am. Acad. Dermatol.* 2005; 53:407–415. [PubMed: 16112345]
17. Foran PG, Mohammed N, Lisk GO, Nagwaney S, Lawrence GW, Johnson E, Smith L, Aoki KR, Dolly JO. Evaluation of the therapeutic usefulness of botulinum neurotoxin B, C1, E, and F compared with the long lasting type A. Basis for distinct durations of inhibition of exocytosis in central neurons. *J. Biol. Chem.* 2003; 278:1363–1371. [PubMed: 12381720]
18. Greenfield RA, Brown BR, Hutchins JB, Iandolo JJ, Jackson R, Slater LN, Bronze MS. Microbiological, biological, and chemical weapons of warfare and terrorism. *Am. J. Med. Sci.* 2002; 323:326–340. [PubMed: 12074487]
19. Rosenbloom M, Leikin JB, Vogel SN, Chaudry ZA. Biological and chemical agents: a brief synopsis. *Am. J. Ther.* 2002; 9:5–14. [PubMed: 11782813]
20. Meunier FA, Lisk G, Sesardic D, Dolly JO. Dynamics of motor nerve terminal remodeling unveiled using SNAP-cleaving botulinum toxins: the extent and duration are dictated by the sites of SNAP-25 truncation. *Mol. Cell Neurosci.* 2003; 22:454–466. [PubMed: 12727443]
21. Lacy DB, Tepp W, Cohen AC, DasGupta BR, Stevens RC. Crystal structure of botulinum neurotoxin type A and implications for toxicity. *Nat. Struct. Biol.* 1998; 5:898–902. [PubMed: 9783750]
22. Simpson LL. Identification of the major steps in botulinum toxin action. *Annu. Rev. Pharmacol. Toxicol.* 2004; 44:167–193. [PubMed: 14744243]
23. Binz T, Blasi J, Yamasaki S, Baumeister A, Link E, Sudhof TC, Jahn R, Niemann H. Proteolysis of SNAP-25 by types E and A botulin neurotoxins. *J. Biol. Chem.* 1994; 269:1617–1620. [PubMed: 8294407]
24. Singh BR. Intimate details of the most poisonous poison. *Nat. Struct. Biol.* 2000; 7:617–619. [PubMed: 10932240]
25. Turton K, Chaddock JA, Acharya KR. Botulinum and tetanus neurotoxins: structure, function and therapeutic utility. *Trends Biochem. Sci.* 2002; 27:552–558. [PubMed: 12417130]

26. Li B, Peet NP, Butler MM, Burnett JC, Moir DT, Bowlin TL. Small molecule inhibitors as countermeasures for botulinum neurotoxin intoxication. *Molecules*. 2011; 16:202–220. [PubMed: 21193845]
27. Schmidt JJ, Stafford RG. A high-affinity competitive inhibitor of type A botulinum neurotoxin protease activity. *FEBS Lett*. 2002; 532:423–426. [PubMed: 12482605]
28. Schmidt JJ, Bostian KA. Proteolysis of synthetic peptides by type A botulinum neurotoxin. *J. Protein Chem*. 1995; 14:703–708. [PubMed: 8747431]
29. Schmidt JJ, Bostian KA. Endoproteinase activity of type A botulinum neurotoxin: substrate requirements and activation by serum albumin. *J. Protein Chem*. 1997; 16:19–26. [PubMed: 9055204]
30. Schmidt JJ, Stafford RG, Bostian KA. Type A botulinum neurotoxin proteolytic activity: development of competitive inhibitors and implications for substrate specificity at the S1' binding subsite. *FEBS Lett*. 1998; 435:61–64. [PubMed: 9755859]
31. Sukonpan C, Oost T, Goodnough M, Tepp W, Johnson EA, Rich DH. Synthesis of substrates and inhibitors of botulinum neurotoxin type A metalloprotease. *J. Pept. Res*. 2004; 63:181–193. [PubMed: 15009541]
32. Burnett JC, Ruthel G, Stegmann CM, Panchal RG, Nguyen TL, Hermone AR, Stafford RG, Lane DJ, Kenny TA, McGrath CF, Wipf P, Stahl AM, Schmidt JJ, Gussio R, Brunger AT, Bavari S. Inhibition of metalloprotease botulinum serotype A from a pseudo-peptide binding mode to a small molecule that is active in primary neurons. *J. Biol. Chem*. 2007; 282:5004–5014. [PubMed: 17092934]
33. Burnett JC, Schmidt JJ, Stafford RG, Panchal RG, Nguyen TL, Hermone AR, Vennerstrom JL, McGrath CF, Lane DJ, Sausville EA, Zaharevitz DW, Gussio R, Bavari S. Novel small molecule inhibitors of botulinum neurotoxin A metalloprotease activity. *Biochem. Biophys. Res. Commun*. 2003; 310:84–93. [PubMed: 14511652]
34. Butler MM, Cardinale SC, Li B, Pai R, Ruthel G, Nuss JE, Wanner LM, Park J-B, Rich C, Basu A, Mills D, Peet NP, Moir D, Bavari S, Bowlin TL. Unpublished results.
35. Li B, Pai R, Cardinale SC, Butler MM, Peet NP, Moir DT, Bavari S, Bowlin TL. Synthesis and Biological Evaluation of Botulinum Neurotoxin A Protease Inhibitors. *J. Med. Chem*. 2010; 53:2264–2276. [PubMed: 20155918]
36. Burnett JC, Li B, Pai R, Cardinale SC, Butler MM, Peet NP, Moir D, Bavari S, Bowlin T. Analysis of botulinum neurotoxin serotype A metalloprotease inhibitors: Analogs of a chemotype for therapeutic development in the context of a three-zone pharmacophore. *Open Access Bioinformatics*. 2010; 2010:11–18. [PubMed: 21103387]
37. Burnett JC, Wang C, Nuss JE, Nguyen TL, Hermone AR, Schmidt JJ, Gussio R, Wipf P, Bavari S. Pharmacophore-guided lead optimization: the rational design of a non-zinc coordinating, sub-micromolar inhibitor of the botulinum neurotoxin serotype A metalloprotease. *Bioorg. Med. Chem. Lett*. 2009; 19:5811–5813. [PubMed: 19703771]
38. Hermone AR, Burnett JC, Nuss JE, Tressler LE, Nguyen TL, Solaja BA, Vennerstrom JL, Schmidt JJ, Wipf P, Bavari S, Gussio R. Three-dimensional database mining identifies a unique chemotype that unites structurally diverse botulinum neurotoxin serotype A inhibitors in a three-zone pharmacophore. *ChemMedChem*. 2008; 3:1905–1912. [PubMed: 19006141]
39. Nuss JE, Dong Y, Wanner LM, Ruthel G, Wipf P, Gussio R, Vennerstrom JL, Bavari S, Burnett JC. Pharmacophore refinement guides the rational design of nanomolar-range inhibitors of the botulinum neurotoxin serotype A metalloprotease. *ACS Med. Chem. Lett*. 2010; 1:301–305. [PubMed: 21116458]
40. Solaja BA, Opsenica D, Smith KS, Milhous WK, Terzic N, Opsenica I, Burnett JC, Nuss J, Gussio R, Bavari S. Novel 4-aminoquinolines active against chloroquine-resistant and sensitive *P. falciparum* strains that also inhibit botulinum serotype A. *J. Med. Chem*. 2008; 51:4388–4391. [PubMed: 18637666]
41. Park JG, Sill PC, Makiyi EF, Garcia-Sosa AT, Millard CB, Schmidt JJ, Pang Y-P. Serotype-selective, small-molecule inhibitors of the zinc endopeptidase of botulinum neurotoxin serotype A. *Bioorg. Med. Chem*. 2006; 14:395–408. [PubMed: 16203152]

42. Tang J, Park JG, Millard CB, Schmidt JJ, Pang YP. Computer-aided lead optimization: improved small-molecule inhibitor of the zinc endopeptidase of botulinum neurotoxin serotype A. *PLoS One*. 2007; 2:e761. [PubMed: 17712409]
43. Pang YP, Vummenthala A, Mishra RK, Park JG, Wang S, Davis J, Millard CB, Schmidt JJ. Potent new small-molecule inhibitor of botulinum neurotoxin serotype A endopeptidase developed by synthesis-based computer-aided molecular design. *PLoS One*. 2009; 4:e7730. [PubMed: 19901994]
44. Boldt GE, Kennedy JP, Janda KD. Identification of a potent botulinum neurotoxin A protease inhibitor using in situ lead identification chemistry. *Org. Lett*. 2006; 8:1729–1732. [PubMed: 16597152]
45. Eubanks LM, Hixon MS, Jin W, Hong S, Clancy CM, Tepp WH, Baldwin MR, Malizio CJ, Goodnough MC, Barbieri JT, Johnson EA, Boger DL, Dickerson TJ, Janda KD. An in vitro and in vivo disconnect uncovered through high-throughput identification of botulinum neurotoxin A antagonists. *Proc. Natl. Acad. Sci. U. S. A.* 2007; 104:2602–2607. [PubMed: 17293454]
46. Capkova K, Hixon MS, Pellett S, Barbieri JT, Johnson EA, Janda KD. Benzylidene cyclopentenediones: First irreversible inhibitors against botulinum neurotoxin A's zinc endopeptidase. *Bioorg. Med. Chem. Lett*. 2009; 20:206–208. [PubMed: 19914829]
47. Eubanks LM, Silhar P, Salzameda NT, Zakhari JS, Xiaochuan F, Barbieri JT, Shoemaker CB, Hixon MS, Janda KD. Identification of a natural product antagonist against the botulinum neurotoxin light chain protease. *ACS Med. Chem. Lett*. 2010; 1:268–272. [PubMed: 20959871]
48. Cardinale SC, Butler MM, Ruthel G, Nuss JE, Wanner LM, Li B, Pai R, Peet NP, Bavari S, Bowlin TL. Novel benzimidazole inhibitors of botulinum neurotoxin/A display enzyme and cell based potency. *The Botulinum J*. 2011; 2:16–29.
49. Schmidt JJ, Stafford RG. Fluorogenic substrates for the protease activities of botulinum neurotoxins, serotypes A, B, and F. *Appl. Environ. Microbiol.* 2003; 69:297–303. [PubMed: 12514008]
50. Panchal RG, Hermone AR, Nguyen TL, Wong TY, Schwarzenbacher R, Schmidt J, Lane D, McGrath C, Turk BE, Burnett J, Aman MJ, Little S, Sausville EA, Zaharevitz DW, Cantley LC, Liddington RC, Gussio R, Bavari S. Identification of small molecule inhibitors of anthrax lethal factor. *Nat. Struct. Mol. Biol.* 2004; 11:67–72. [PubMed: 14718925]
51. Adam GC, Cravatt BF, Sorensen EJ. Profiling the specific reactivity of the proteome with non-directed activity-based probes. *Chem. Biol.* 2001; 8:81–95. [PubMed: 11182321]
52. Zhao Y, Jensen ON. Modification-specific proteomics: strategies for characterization of post-translational modifications using enrichment techniques. *Proteomics*. 2009; 9:4632–4641. [PubMed: 19743430]
53. Breidenbach MA, Brunger AT. Substrate recognition strategy for botulinum neurotoxin serotype A. *Nature*. 2004; 432:925–929. [PubMed: 15592454]
54. Scott CJ, McDowell A, Martin SL, Lynas JF, Vandenbroeck K, Walker B. Irreversible inhibition of the bacterial cysteine protease-transpeptidase sortase (SrtA) by substrate-derived affinity labels. *Biochem. J*. 2002; 366:953–958. [PubMed: 12069686]
55. Kim JR, Yoon HW, Kwon KS, Lee SR, Rhee SG. Identification of proteins containing cysteine residues that are sensitive to oxidation by hydrogen peroxide at neutral pH. *Anal. Biochem*. 2000; 283:214–221. [PubMed: 10906242]
56. Singh J, Petter RC, Kluge AF. Targeted covalent drugs of the kinase family. *Curr. Opin. Chem. Biol.* 2010; 14:475–480. [PubMed: 20609616]
57. Hagel M, Niu D, St Martin T, Sheets MP, Qiao L, Bernard H, Karp RM, Zhu Z, Labenski MT, Chaturvedi P, Nacht M, Westlin WF, Petter RC, Singh J. Selective irreversible inhibition of a protease by targeting a noncatalytic cysteine. *Nat. Chem. Biol.* 2010; 7:22–24. [PubMed: 21113170]
58. Waterson AG, Petrov KG, Hornberger KR, Hubbard RD, Sammond DM, Smith SC, Dickson HD, Caferro TR, Hinkle KW, Stevens KL, Dickerson SH, Rusnak DW, Spehar GM, Wood ER, Griffin RJ, Uehling DE. Synthesis and evaluation of aniline headgroups for alkynyl thienopyrimidine dual EGFR/ErbB-2 kinase inhibitors. *Bioorg. Med. Chem. Lett*. 2009; 19:1332–1336. [PubMed: 19208477]

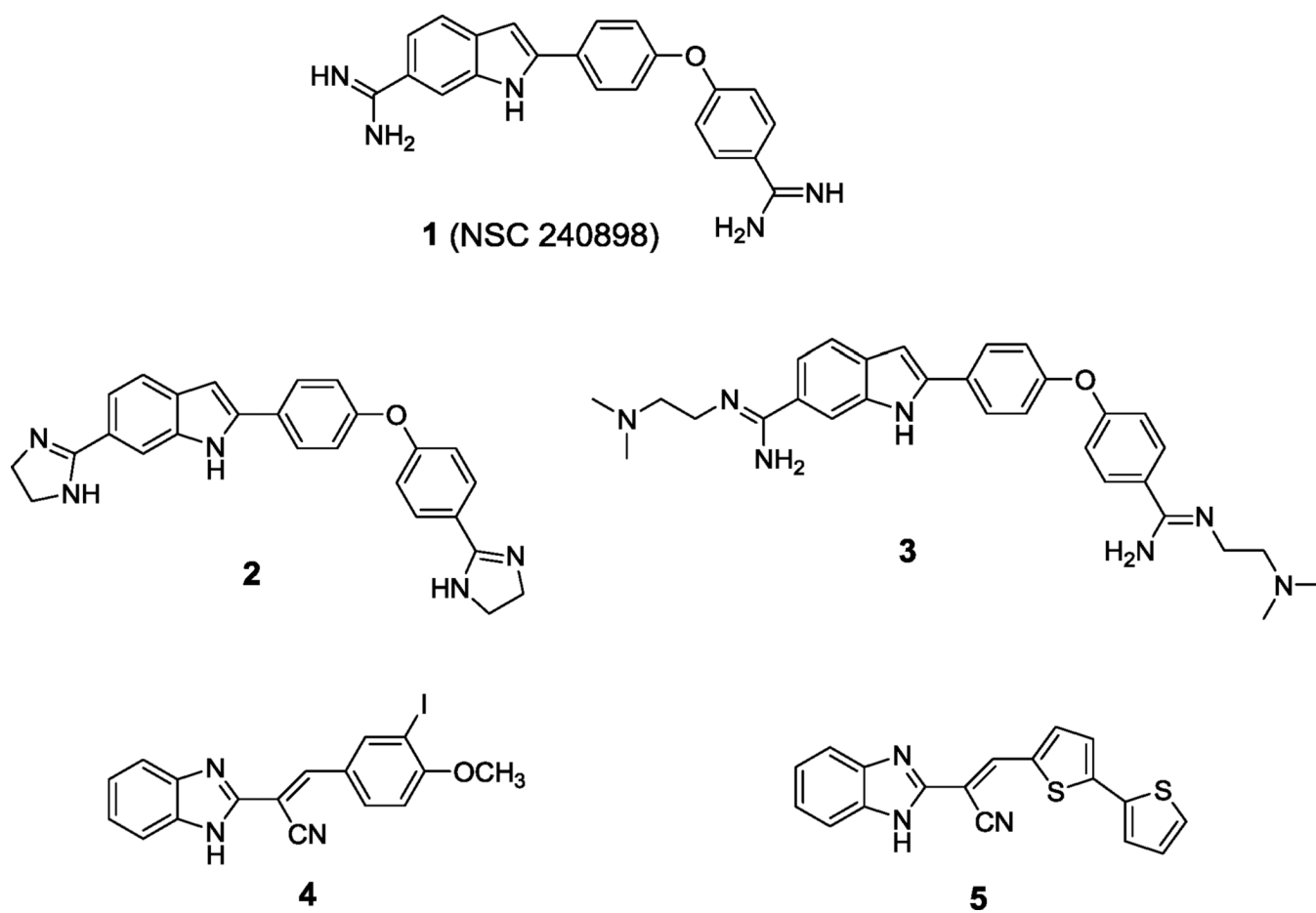
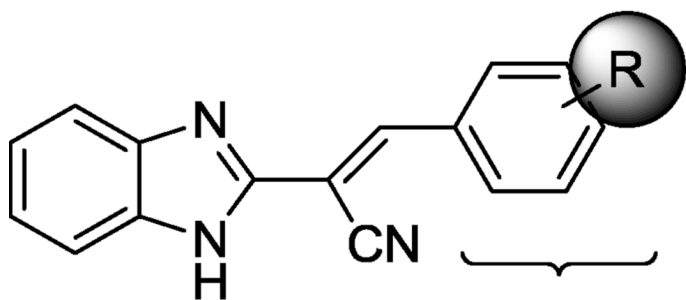


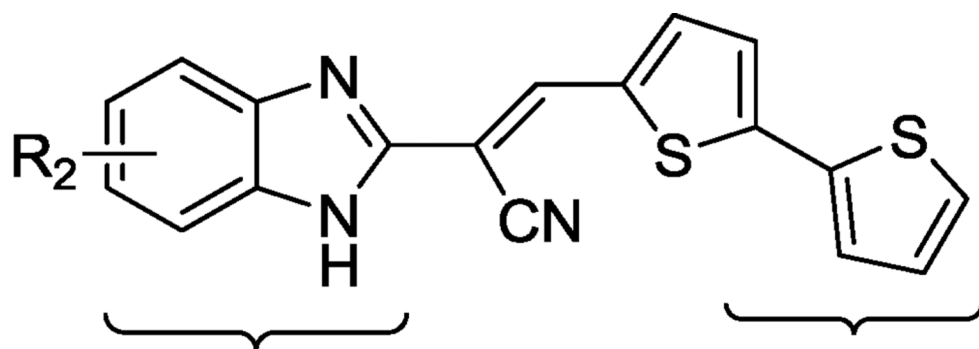
Figure 1.
Structures of BoNT/A LC inhibitors.

mono-, di-, tri-substitutions



heteroaromatic ring replacement

Figure 2.
Modifications of the hit structure 4.



core replacement

substituent replacement

Figure 3.
Modification of compound 5.

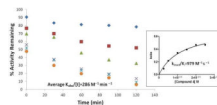


Figure 4.
Inactivation of BoNT/A LC with compound 4.

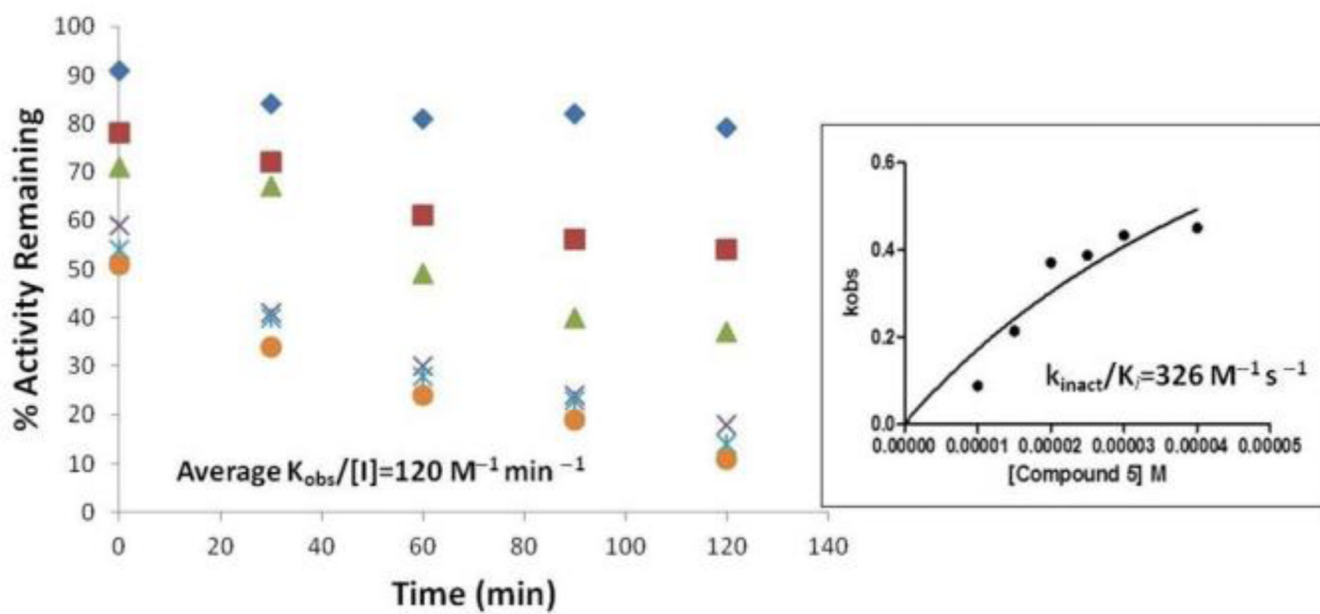


Figure 5.
Inactivation of BoNT/A LC with compound 5.

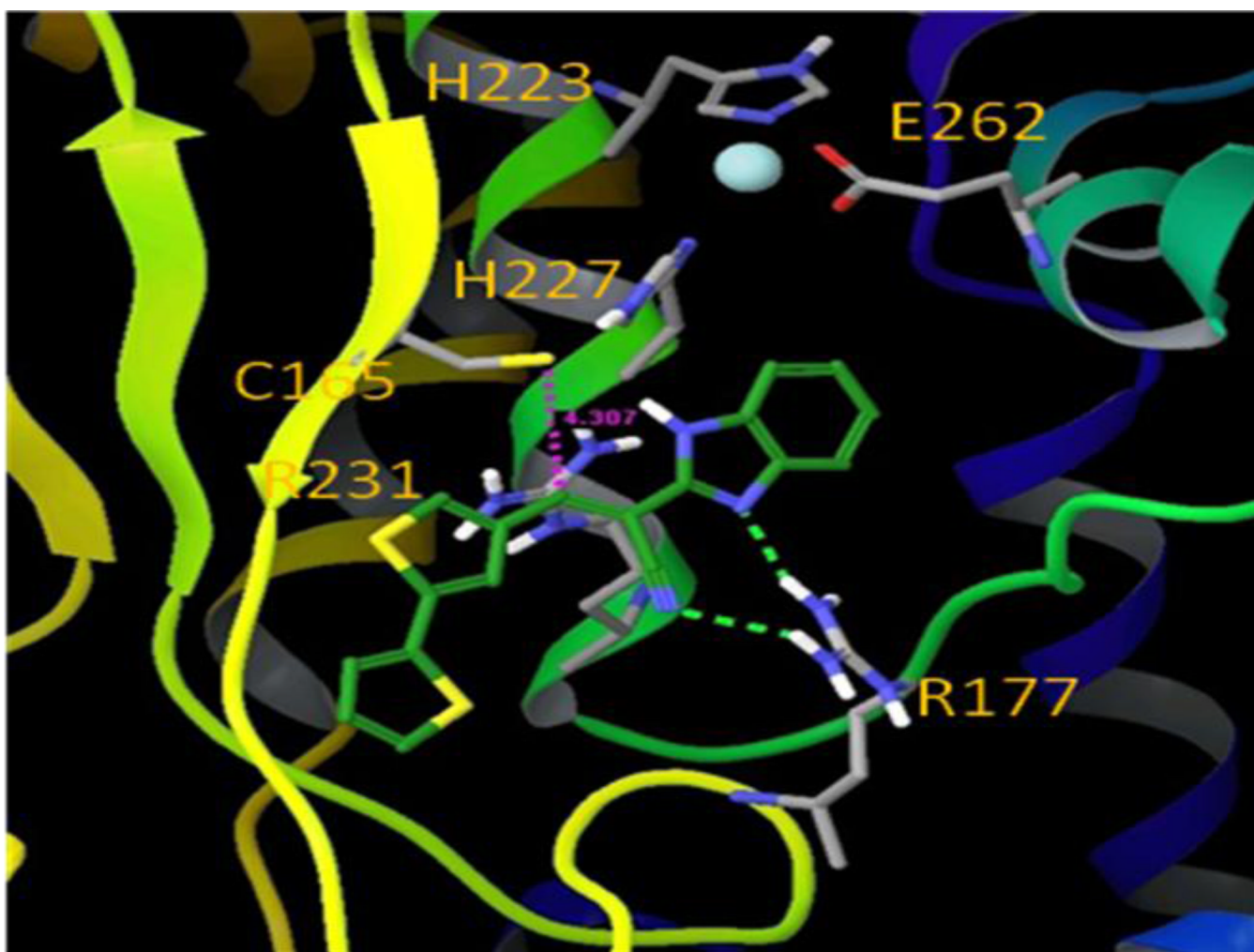


Figure 7.
Compound 5 non-covalently bound near the C165 site (T-exosite).

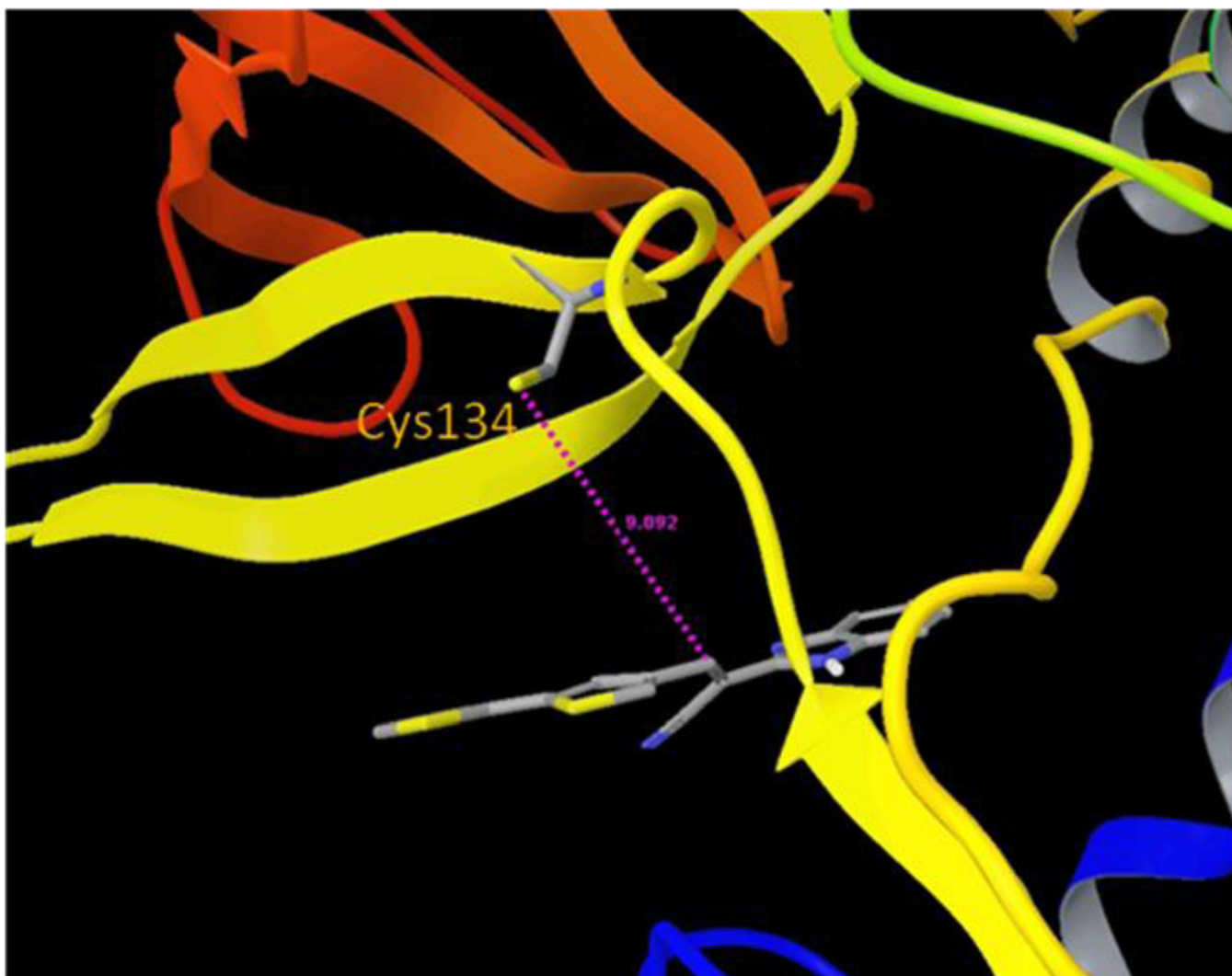


Figure 8.
Molecular model of compound **5** in the Cys134 site of BoNT/A LC.

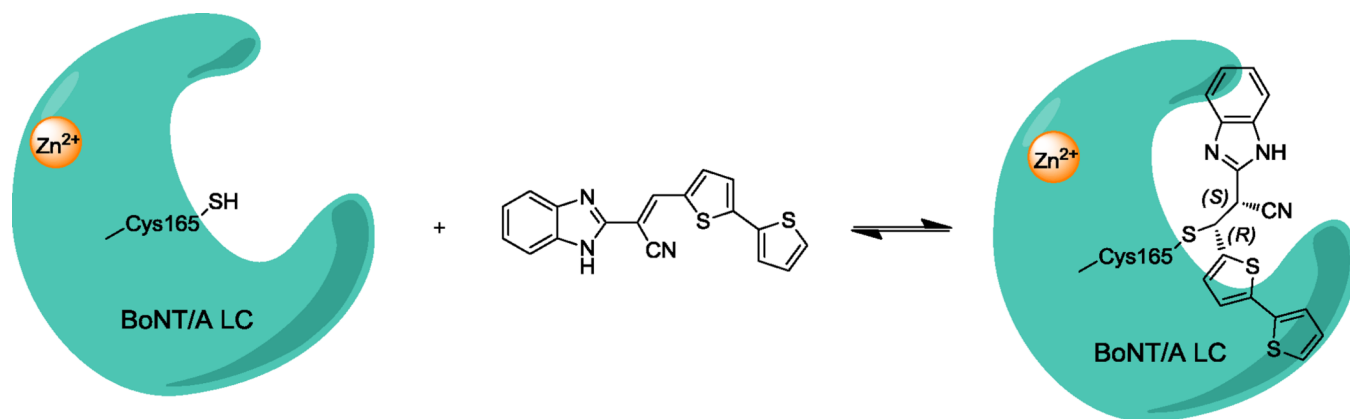


Figure 9. Compound **5** is proposed to inactivate BoNT/A LC by forming a covalent bond with Cys165.

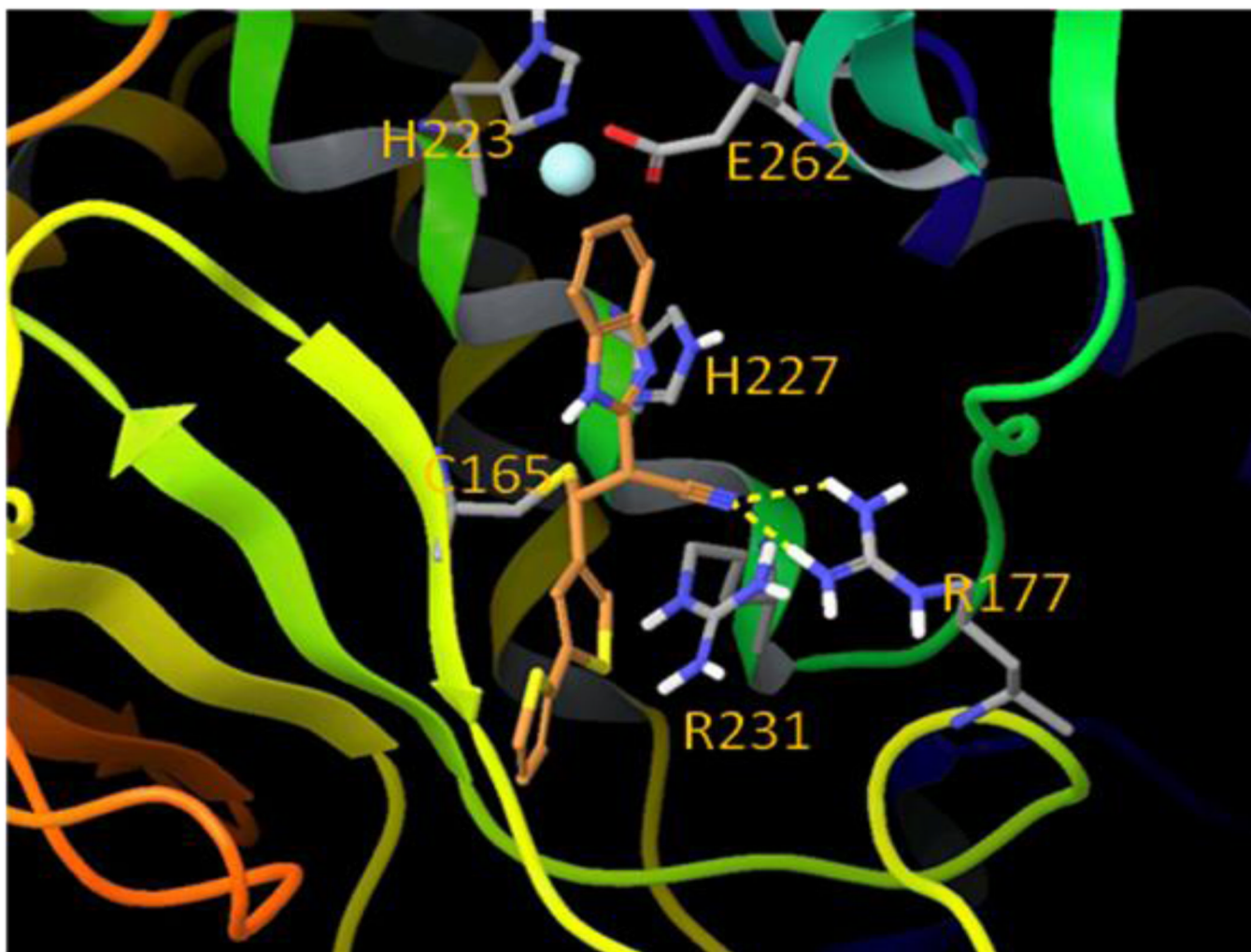
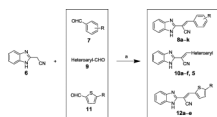
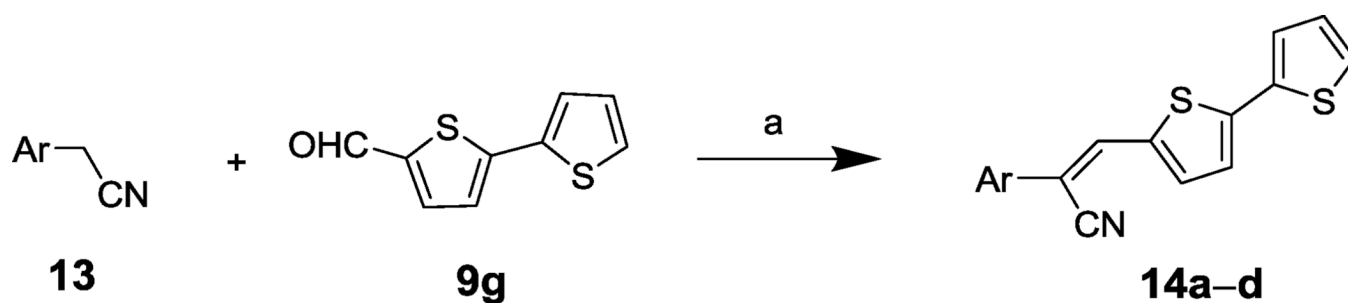


Figure 10.
Compound **5** covalently bound at the Cys165 site (T-exosite).

**Scheme 1.**

Syntheses of benzimidazole acrylonitriles **8a–k**, **10a–f**, **5**, and **12a–e**.^a Reagents and conditions: (a) NaOAc, HOAc, reflux, 2h.



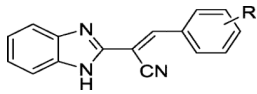
Ar = 2-indolyl, 2-benzothiazolyl,
2-benzoxazinyl, 2-quinolinyl

Scheme 2.

Syntheses of **14a-d**. ^a Reagents and conditions: (a) NaOAc, HOAc, reflux, 2h.

Table 1

Inhibitory activities of benzimidazole acrylonitriles **4**, **8a–8k** against BoNT/A LC and LF enzymes.

			
Compound	R	^a BoNT/A LC IC ₅₀ (μM)	^b Anthrax LF IC ₅₀ (μM)
4	3-I, 4-OMe	7.2/10 ^c	74
8a	3-I	>100	>100
8b	3-H, 4-OMe	>100	>100
8c	3-Br, 4-OMe	>100	>100
8d	3-Cl, 4-OMe	>100	>100
8e	3-F, 4-OMe	>100	>100
8f	3,4-di-OMe	>100	>100
8g	3-Cl, 4-OH, 5-OMe	59	>100
8h	3-Br, 4-OH, 5-OMe	94	>100
8i	4-Ph	86	>100
8j	4-Imidazole	73	>100
8k	3,4,5-tri-OMe	>100	>100

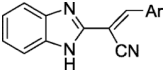
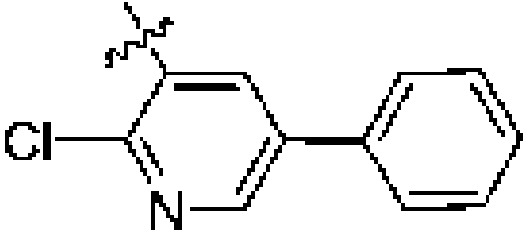
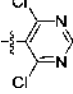
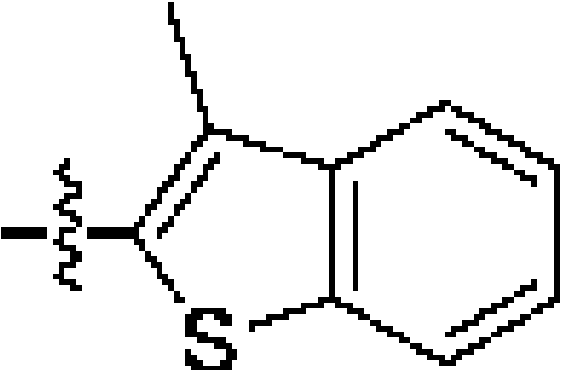
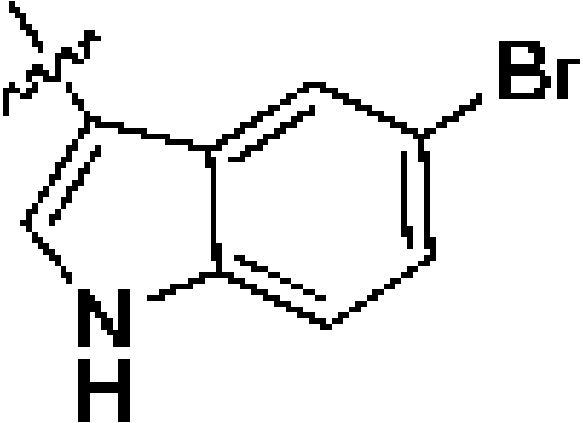
^aResults obtained by average of two experiments in a FRET assay;

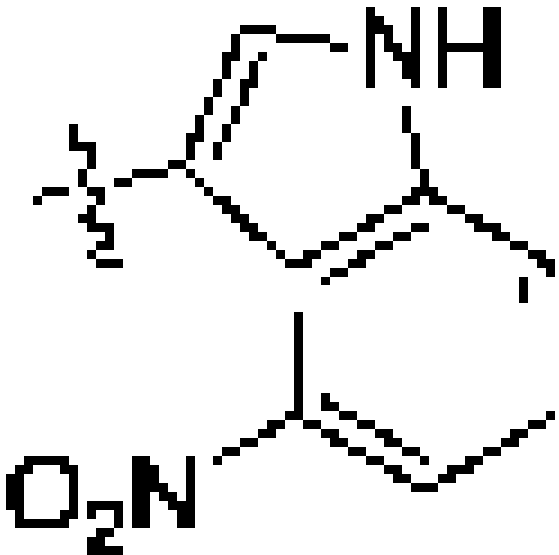
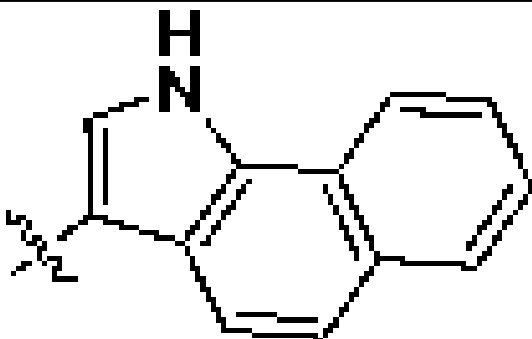
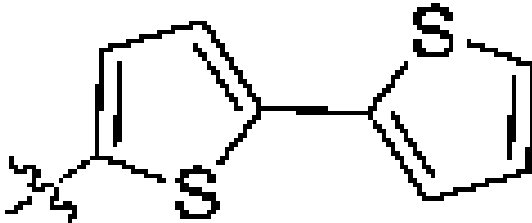
^bresults obtained by FRET assay;

^cresults obtained by HPLC assay.

Table 2

Inhibitory activities of benzimidazole acrylonitriles **10a–f** against BoNT/A LC and LF enzymes.

Compound	Ar		
		^a BoNT/A LC IC ₅₀ (μM)	^b Anthrax LF IC ₅₀ (μM)
10a		>100	>100
10b		>100	>100
10c		>100	>100
10d		>100	60% inh. @100μM

Compound	Ar	^a BoNT/A LC IC ₅₀ (μM)	^b Anthrax LF IC ₅₀ (μM)
10e		>100	>100
10f		>100	>100
5		26 (29 ^c)	>100

^a Results obtained by average of two experiments in a FRET assay;

^b results obtained by FRET assay;

^c results obtained by HPLC assay.

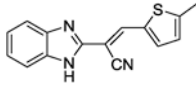
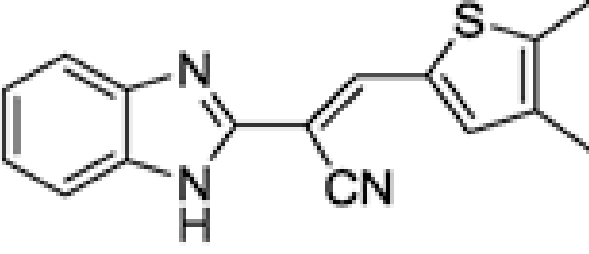
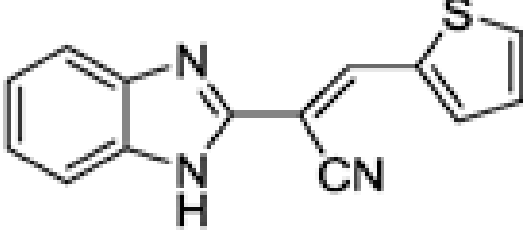
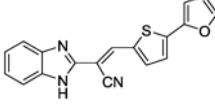
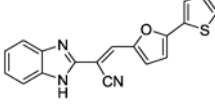
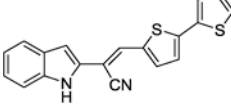
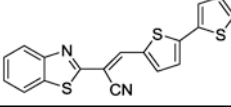
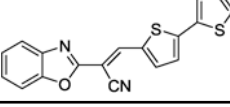
Table 3*In vitro* characterization of compounds **4** and **5**.

	Compound 4	Compound 5
Assay	IC ₅₀ (μM) or %inhibition	IC ₅₀ (μM) or %inhibition
BoNT/A LC FRET	7.2	26
BoNT/A LC HPLC	10	29
BoNT/B LC FRET	>100	>100
<i>Anthrax</i> LF	74	>100
MMP-1	>100	>100
MMP-2	>100	>100
MMP-9	>100	>100
% Inhibition@30μM chick neuronal assay	<10% Inhibition	59% Inhibition
Inactivated by zinc chelation	No	No
Inactivated by glutathione	Yes	No
Inactivated by cysteine	Yes	No

^aInactivation studies were performed by pre-incubating the potential inactivator (at 2.5 or 5 mM) with compound in the assay mixture for 15 minutes at 37 °C and then adding the 17-mer SNAP-25 substrate and BoNT/A LC.

Table 4

Inhibitory activities of compounds **12a–e**, **14a–d**, and **15** against BoNT/A LC and LF enzymes.

Compound	Ar	^a BoNT/A LC IC ₅₀ (μM)	^b LF IC ₅₀ (μM)
12a		>100	>100
12b		>100	>100
12c		>100	>100
12d		59	>100
12e		>100	>100
14a		>100	>100
14b		>100	>100
14c		>100	N.D.

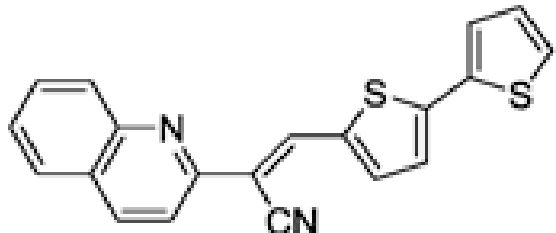
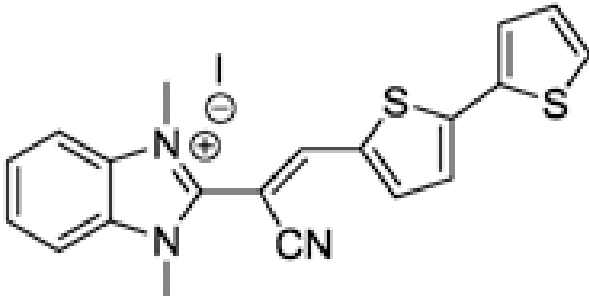
Compound	Ar	^a B ₀ NT/A LC IC ₅₀ (μM)	^b LF IC ₅₀ (μM)
14d		>100	>100
15		>100	N.D.

Table 5

Enzyme/Inhibitor “Rescue” studies.

Experimental Condition	Activity Remaining (Fraction of Dialyzed Control)
50 μ M 5	0.55
50 μ M 4	0.17
50 μ M 2	1.25
50 μ M 5/50 μ M 2	1.13
50 μ M 4/50 μ M 2	0.99